

# A sensitive monitoring system for mammalian cell cultivation processes: a PAT approach

Silvia Winckler · Rolf Krueger · Thomas Schnitzler ·  
Werner Zang · Rainer Fischer · Manfred Biselli

Received: 4 August 2013 / Accepted: 9 September 2013  
© Springer-Verlag Berlin Heidelberg 2013

**Abstract** Biopharmaceuticals such as antibodies are produced in cultivated mammalian cells, which must be monitored to comply with good manufacturing practice. We, therefore, developed a fully automated system comprising a specific exhaust gas analyzer, inline analytics and a corresponding algorithm to precisely determine the oxygen uptake rate, carbon dioxide evolution rate, carbon dioxide transfer rate, transfer quotient and respiratory quotient without interrupting the ongoing cultivation, in order to assess its reproducibility. The system was verified using chemical simulation experiments and was able to measure the respiratory activity of hybridoma cells and DG44 cells (derived from Chinese hamster ovary cells) with satisfactory results at a minimum viable cell density of  $\sim 2.0 \times 10^5$  cells  $\text{ml}^{-1}$ . The system was suitable for both batch and fed-batch cultivations in bubble-aerated and

membrane-aerated reactors, with and without the control of pH and dissolved oxygen.

**Keywords** Batch-to-batch reproducibility · Bicarbonate-buffered media · Carbon dioxide evolution rate · Mammalian cells · Monitoring · Oxygen uptake rate

## Abbreviations

$a_{\text{CO}_2}$	Activity of carbon dioxide (–)
$a_{\text{H}^+}$	Activity of hydrogen ion (–)
$a_{\text{HCO}_3^-}$	Activity of hydrogen carbonate (–)
CER	Carbon dioxide evolution rate ( $\text{mol l}^{-1} \text{h}^{-1}$ )
$c_i$	Molar concentration of an ion ( $\text{mol l}^{-1}$ )
$c_{\text{CO}_2,0}$	Saturation concentration of carbon dioxide at the boundary layer of the gas phase ( $\text{mol l}^{-1}$ )
$c_{\text{CO}_2,g}$	Molar concentration of carbon dioxide in the gas phase ( $\text{mol l}^{-1}$ )
$c_{\text{CO}_2,l}$	Molar concentration of carbon dioxide in the liquid phase ( $\text{mol l}^{-1}$ )
$c_{\text{HCO}_3^-}$	Molar concentration of hydrogen carbonate ( $\text{mol l}^{-1}$ )
$c_{\text{IC}}$	Total molar concentration of inorganic carbon ( $\text{mol l}^{-1}$ )
$c_{\text{IC},t1}$	Molar concentration of inorganic carbon at time one ( $\text{mol l}^{-1}$ )
$c_{\text{IC},t2}$	Molar concentration of inorganic carbon at time two ( $\text{mol l}^{-1}$ )
CT	Total carbon dioxide transfer ( $\text{mol l}^{-1}$ )
CTR	Carbon dioxide transfer rate ( $\text{mol l}^{-1} \text{h}^{-1}$ )
$c^*$	Saturation concentration of carbon dioxide ( $\text{mol l}^{-1}$ )

S. Winckler · T. Schnitzler · M. Biselli (✉)  
Institute of Nano and Biotechnologies (INB), FH Aachen  
University of Applied Sciences, Campus Jülich, Heinrich-  
Mubmann-Str.1, 52428 Jülich, Germany  
e-mail: biselli@fh-aachen.de

S. Winckler  
e-mail: Winckler@fh-aachen.de

R. Krueger · W. Zang  
HiTec Zang GmbH, Ebertstr. 30-32, 52134 Herzogenrath,  
Germany

R. Fischer  
Fraunhofer Institute for Molecular Biology and Applied  
Ecology, Forckenbeckstr. 6, 52074 Aachen, Germany

R. Fischer  
Institute for Molecular Biotechnology, RWTH Aachen  
University, Worringerweg 1, 52074 Aachen, Germany

$\frac{dc_{ic}}{dt}$	Variation of inorganic carbon concentration in one period ( $\text{mol l}^{-1} \text{h}^{-1}$ )
$H_{CO_2}$	Henry constant for carbon dioxide ( $\text{mol l}^{-1} \text{bar}^{-1}$ )
$I$	Ionic strength ( $\text{mol l}^{-1}$ )
$k_L a_{CO_2}$	Volume-specific carbon dioxide mass transfer coefficient ( $\text{h}^{-1}$ )
$K_S$	Mass action constant ( $\text{mol l}^{-1}$ )
OTR	Oxygen transfer rate ( $\text{mol l}^{-1} \text{h}^{-1}$ )
OUR	Oxygen uptake rate ( $\text{mol l}^{-1} \text{h}^{-1}$ )
$p_{\text{ambient}}$	Ambient pressure (bar)
$p_{CO_2, \text{Ferm}}$	Partial pressure of carbon dioxide in the liquid phase of the bioreactor (bar)
RQ	Respiratory quotient (–)
$T$	Temperature (K)
$TI_{\text{headspace}}$	Time delay caused by headspace of the bioreactor (h)
TQ	Transfer quotient (–)
$t$	Time (h)
$t_P$	Process time (h)
$\tau$	Delay time (h)
$V_{\text{culture volume}}$	Culture volume in the bioreactor (l)
$\dot{V}_{\text{inlet, gas}}$	Inlet gas flow rate ( $\text{l h}^{-1}$ )
$V_m$	Molar gas volume ( $\text{mol l}^{-1}$ )
$x_{CO_2, \text{in}}$	Molar fraction of carbon dioxide in the inlet gas (%)
$x_{CO_2, \text{out}}$	Molar fraction of carbon dioxide in the off-gas (%)
$x_{O_2, \text{in}}$	Molar fraction of oxygen in the inlet gas (%)
$x_{O_2, \text{out}}$	Molar fraction of oxygen in the off-gas (%)
$x_{O_2, \text{out, averaged}}$	Average molar fraction of oxygen in the off-gas (%)
$X_{PT1, n}$	Value of time point n (depends on step response)
$X_{PT1, n-1}$	Value of time point n-1 (depends on step response)
$X_{\text{step}}$	Current value of step response (depends on step response)
$\delta_{HCO_3^-}$	Activity coefficient of hydrogen carbonate (–)
$\zeta$	Flow rate correction factor (–)

## Introduction

One of the key requirements of both good manufacturing practice (GMP) and the FDA process analytical technology (PAT) initiative is to ensure the consistent quality of glycosylated biopharmaceutical proteins such as antibodies and the robustness of the production process [11]. Biopharmaceutical manufacturing processes must therefore

achieve sufficient batch-to-batch reproducibility to meet these needs, which requires careful monitoring of mammalian cell culture processes [1, 17, 28]. Three different methods are available for this purpose:

First, the production processes can be monitored off-line/at-line, also known as ex situ analysis. Here, a sample is removed from the bioreactor and analyzed separately, which allows the measurement of a large number of parameters although with a residual risk of bioprocess contamination and no possibility of automated feedback control for fed-batch cultivations.

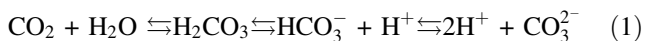
Second, the production processes can be monitored online/inline, also known as in situ analysis. In this case, a measuring device such as an electrode is inserted directly into the liquid phase of the bioreactor, either within the bioreactor vessel or in a separate chamber with access via bypass. Thereby taking a sample is advantageously not necessary so the contamination risk is decreased. Furthermore, the analysis is carried out in real time whereby data can be used not only to monitor the cultivation but also to achieve feedback control. However, only a small number of parameters can be measured.

Finally, production processes can be monitored using non-invasive methods to observe the oxygen and carbon dioxide concentrations in the inlet gas and off-gas (exhaust gas) stream outside the sterile barrier, e.g., mass spectrometry, gas chromatography or typical exhaust gas analysis [2, 8, 12, 19, 20]. This technique provides the ability to determine the oxygen uptake rate (OUR) and the carbon dioxide evolution rate (CER) without interrupting the ongoing process. Non-invasive monitoring can be effective if the properties of the experimental setup discussed below are taken into account:

Mammalian cells have a low respiratory activity which means that differences between the inlet gas and off-gas concentrations are small and difficult to measure [18, 20]. Highly sensitive  $O_2$  and  $CO_2$  detectors are therefore required with an accurate signal-to-noise ratio [12].

Moreover it is necessary to consider the headspace, which introduces a delay in the off-gas stream. Hence, the inlet gas concentration cannot be compared to the off-gas stream without the regard of a defined correction factor [7]. If this time lag is neglected, the OUR, CER and carbon dioxide transfer rate (CTR) cannot be estimated. Without considering the time lag also the volume-specific mass transfer coefficient ( $k_L a$ ) cannot be determined from the exhaust gas analyzer data, which is necessary to calculate the CER.

Another challenge is related to sodium bicarbonate ( $NaHCO_3$ ) containing medium that is usually used in mammalian cell culture. When lactic acid is produced by the cells, protons are released into the liquid phase of the bioreactor by dissociation, which directly affects the carbonate system as shown in Eq. 1.



Under working conditions, the simplified reaction scheme shown below can be used because in the normal cultivation pH range (6.9–7.5), the amount of carbonic acid and carbonate in the liquid phase is negligible [8, 12].



Nevertheless, buffer-released  $\text{CO}_2$  is stripped out into the bioreactor headspace and is measured along with the respiratory  $\text{CO}_2$  in the exhaust gas. For this reason it is impossible to distinguish between biologically produced and buffer-released  $\text{CO}_2$  by non-invasive analysis without an algorithm to correct for the presence of bicarbonate in the medium [3, 8, 12, 19, 20]. But due to the fact that  $\text{NaHCO}_3$  is required as a substrate abdication of bicarbonate has a detrimental impact on the cells behavior and performance. In addition, the absence of this substrate also affects the osmolality of the medium [8].

To address these mentioned challenges, we developed an automated measurement system that allows mammalian cell cultures to be monitored in real time by combining inline and non-invasive analysis. This new system is compatible with different cultivation modes and bioreactor types and provides a practical approach to monitor bio-manufacturing processes using mammalian cells.

## Materials and methods

### Cells and media

The IgG-secreting mouse–mouse hybridoma cell line CF-10H5 (German Collection of Microorganisms and Cell Culture, DSMZ) was cultured in DMEM/Ham's F12 (2:1) powder medium supplemented with 6 mM glutamine, 28.6 mM  $\text{NaHCO}_3$ , 3 mM HEPES, 16 mM glucose and 1 % (v/v) fetal calf serum. The Chinese hamster ovary (CHO) derived cell line DG44 was cultured in commercial Lonza AG PowerCHO2 and Lonza AG ProCHO4 media, with Lonza AG Power Feed A included as a feeding solution. The DG44 cell line was previously transfected to produce a recombinant antibody and adapted to grow in suspension by Anne Peuscher (Fraunhofer IME, Aachen, Germany). The cells were transferred to T25 flasks after thawing, passaged in T75 flasks and maintained in spinner flasks in a humidified incubator at 37 °C with a 5 %  $\text{CO}_2$  atmosphere. A 300-ml pre-culture volume was used to inoculate the bioreactor with a cell density of  $1.5\text{--}2.5 \times 10^5$  viable cells  $\text{ml}^{-1}$ . No antibiotics were used in any of the experiments.

### Bioreactor

Batch and fed-batch processes were carried out in a 2.5-l stirred tank bioreactor with a working volume of 1.8 l. Fed-batch processes had thereby an initial volume of 0.8 l. The vessel was equipped with a double jacket to maintain the process at 37 °C and an exhaust gas cooling system (Biostat A, Sartorius-Stedim Biotech). The culture was stirred at 150 rpm using two dual-blade paddle stirrers. The inlet gas flow rate was maintained at  $3.6 \text{ l h}^{-1}$  (0.033 vvm). With the exception of one bubble-aerated culture, the bioreactor was aerated using a 5-m silicone membrane tube with an internal diameter of 4 mm and an external diameter of 5 mm, which was fully submerged in the culture medium. The silicone tube ended in the headspace of the fermenter as described by Ducommun et al. [10]. The pH of the medium was measured using a glass electrode (Steamline, SI-Analytics) with a resolution of 0.001 between measuring points (not the absolute resolution). The dissolved oxygen (DO) was determined using an optical probe (VisiFerm DO, Hamilton GmbH) and the temperature was observed and controlled with a standard Pt 100 temperature sensor. Cultivation processes were established with and without pH and DO control. In case of non-controlled cultivations, the inlet flow comprised a 19:76:5 mixture of  $\text{O}_2$ ,  $\text{N}_2$  and  $\text{CO}_2$ . During a pH- and DO-controlled process the pH was maintained at 7.2 by  $\text{CO}_2$  addition/minimization (PI element) and the addition of 0.5 M NaOH (P element). The dissolved oxygen was maintained at 35 % air saturation (PI element). The data were collected by LabVision® (HiTec Zang GmbH) and graphical presentation was prepared using Excel 2010.

### HiSense™ measurement system

The measurement system (HiSense™ with corresponding algorithm, which is commercially available) was developed in collaboration with HiTec Zang GmbH.

To meet the requirements of mammalian cell cultivations, the analyzer comprised two sensors each for oxygen and  $\text{CO}_2$ . The gas stream was multiplexed, so one probe measured the concentration in both the inlet gas and the off-gas stream, thus minimizing the impact of drift on the results. The differential measurement ensured that even calibration faults had no decisive impact on performance. The oxygen concentration was determined using a solid electrolyte sensor ( $\text{ZrO}_2$ ) in prototype I and a paramagnetic sensor in prototype II (Table 1). Thereby the sensors differ only in their technical way of measuring  $\text{O}_2$  not affecting the realized OTR/OUR results. The  $\text{CO}_2$  concentration was determined using a non-dispersive infrared (NDIR) sensor in both analyzers.

**Table 1** Technical characteristics of the used sensors

Gas	Sensor	Range (vol %)	Uncertainty (vol %)	Resolution (vol %)
Oxygen	ZnO <sub>2</sub>	0–30 30–100	1	0.02
Oxygen	Paramagnetic	0–100	1	0.02
Carbon dioxide	NDIR	0–20	0.5	0.05

After compensation for humidity and pressure, the differential measurement had a resolution of  $\sim 0.005$  vol %. The analyzer (with internal H<sub>2</sub>O drying system) was connected to the bioreactor behind the exhaust gas cooling system via low-permeability polyether ether ketone (PEEK) gas tubes (CS Chromatography GmbH) with small internal diameters (0.75 mm) to limit the dead volume [12, 29]. A measuring value was recorded at 8-min intervals.

### Analytical methods

Culture samples (8–9 ml) were taken once or twice daily for off-line analysis. Viable cell concentrations were determined by hemocytometer (Marienfeld) counts with Erythrosin B and Casy<sup>®</sup>TT.

### Feeding strategy of the fed-batch process

Feeding during the fed-batch process depended on the availability of glucose in the cell suspension. Assuming that lactic acid was produced when glucose was available in excess, feeding was only valid when NaOH, provided for pH maintenance, was not required. If lactic acid was produced, NaOH was needed to maintain the pH and feeding was withheld, whereas nutrients were provided if NaOH was not required [16]. Therefore, this mechanism was programmed in LabVision<sup>®</sup> using the following relationship (Fig. 1).

### Theoretical aspects and mathematical algorithm

During cultivation, mammalian cells consume oxygen and produce carbon dioxide at rates known as oxygen uptake rate (OUR) and carbon dioxide evolution rate (CER). The OUR can easily be determined with an exhaust gas analyzer using a global mass balance, if the headspace of the bioreactor is compared to an accumulator of the first order. Therefore, we used a simplified assumption to deal with this difficulty. A time-discrete PT1 element, which is normally used in digital signal processing [24], was applied the first time to model the step response of the off-gas value (Eq. 3) in the mathematical algorithm of our new analytical system.

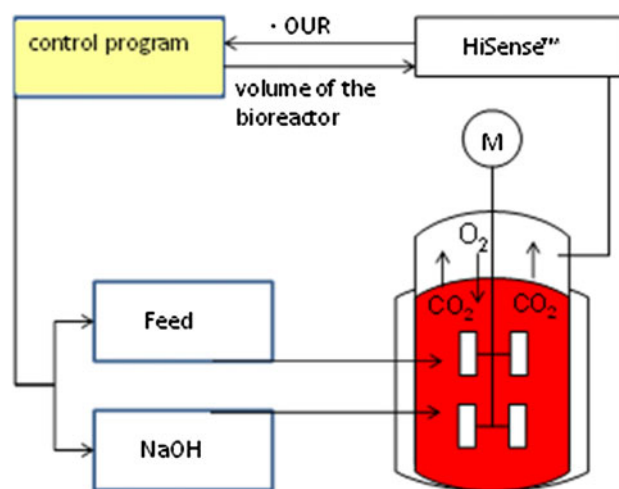


**Fig. 1** Feeding strategy. The OUR value obtained from the analyzer was used for feed control. Assuming that six oxygen molecules were necessary for oxidative metabolism of one glucose molecule resulting in 50 % biomass formation out of this molecule, 33 % of the OUR value were continuously fed as feed solution if pumping was valid

$$X_{\text{step}} = \left( \frac{\tau}{\Delta t} + 1 \right) \times X_{\text{PT1},n} - \frac{\tau}{\Delta t} \times X_{\text{PT1},n-1} \quad (3)$$

The equation above can be rearranged to approximately reconstruct the original step response for O<sub>2</sub> concentration (analog signal processing for CO<sub>2</sub>) in the bioreactor headspace and thus in the off-gas vent line (Eq. 4)

$$x_{\text{O}_2,\text{out}} = \left( \frac{T1_{\text{headspace}}}{\Delta t} + 1 \right) \times x_{\text{O}_2,\text{out,averaged}} - \frac{T1_{\text{headspace}}}{\Delta t} \times x_{\text{O}_2,\text{out,averaged}-1} \quad (4)$$

Subsequently, the inlet and off-gas concentrations of O<sub>2</sub> are used to determine the oxygen transfer rate (OTR) in Eq. 5. Under steady-state conditions, the OTR is equal to the OUR [12, 23].

$$\text{OTR} = \frac{\dot{V}_{\text{inletgas}}}{V_m \cdot V_{\text{culturevolume}}} \cdot (x_{\text{O}_2,\text{in}} - \zeta \cdot x_{\text{O}_2,\text{out}}) \quad (5)$$

$$\zeta = \frac{100 - x_{\text{O}_2,\text{in}} - x_{\text{CO}_2,\text{in}}}{100 - x_{\text{O}_2,\text{out}} - x_{\text{CO}_2,\text{out}}} \quad (6)$$

Compared to OUR, CER is not as simple to calculate because of the presence of NaHCO<sub>3</sub>, which means that the CER is not equivalent to CTR. Nevertheless, the CTR is required to calculate the CER by considering quantitative changes in the inorganic carbon pool over time ( $d_{\text{IC}}/d_t$ ) as previously described by Neeleman et al. [19].

$$\text{CTR} = \frac{\dot{V}_{\text{inletgas}}}{V_m \cdot V_{\text{culturevolume}}} \cdot (x_{\text{CO}_2,\text{out}} \cdot \zeta - x_{\text{CO}_2,\text{in}}) \quad (7)$$

$$\text{CER} = \text{CTR} - \frac{dc_{\text{IC}}}{dt} \quad (8)$$

$$\frac{d_{\text{IC}}}{dt} = \frac{c_{\text{IC},t2} - c_{\text{IC},t1}}{t_2 - t_1} \quad (9)$$

The total concentration of inorganic carbon  $c_{\text{IC}}$  comprises the bicarbonate fraction  $c_{\text{HCO}_3^-}$ , the  $\text{CO}_2$  fraction in the liquid phase  $c_{\text{CO}_2,l}$  and in the gas phase  $c_{\text{CO}_2,g}$  where the activity of bicarbonate ( $a_{\text{HCO}_3^-}$ ) is derived using the modified law of mass action:

$$c_{\text{IC}} = c_{\text{HCO}_3^-} + c_{\text{CO}_2,l} + c_{\text{CO}_2,g} \quad (10)$$

$$c_{\text{HCO}_3^-} = \frac{a_{\text{HCO}_3^-}}{\delta_{\text{HCO}_3^-}} \quad (11)$$

$$a_{\text{HCO}_3^-} = \frac{K_S \times a_{\text{CO}_2}}{a_{\text{H}^+}} \quad (12)$$

The activity of  $\text{CO}_2$  ( $a_{\text{CO}_2} = 1$ ) is therefore also equal to  $c_{\text{CO}_2,l}$  in the liquid phase. The following context allows the calculation of  $a_{\text{CO}_2}$ :

$$a_{\text{CO}_2} = H_{\text{CO}_2} \times p_{\text{CO}_2,\text{Ferm}} \quad (13)$$

where the Henry constant (H) is corrected for both temperature and substance as described by Binder et al. [5] and Deckwer and Schumpe [9]

$$c_{\text{CO}_2,l} = \frac{\text{CTR}}{k_L a_{\text{CO}_2}} + c_{\text{CO}_2,0} \quad (14)$$

With the help of a modified CTR equation including the  $k_L a$  of  $\text{CO}_2$  and global mass balancing, it is possible to estimate the saturation concentration of  $\text{CO}_2$  at the boundary layer of the gas phase ( $c_{\text{CO}_2,0}$ ), which allows the partial pressure in the liquid phase ( $p_{\text{CO}_2,\text{Ferm}}$ ) to be estimated based on the correlation between the  $\text{CO}_2$  concentration and the partial pressure.

The individual activity coefficient of bicarbonate ( $\delta_{\text{HCO}_3^-}$ ) can be determined as described by Davis [27].

The  $\text{CO}_2$  concentration in the gas phase was estimated using the following equation:

$$c_{\text{CO}_2,g} = \frac{x_{\text{CO}_2,\text{out}}}{100 \times V_m \times V_{\text{culture volume}}} \quad (15)$$

If these calculations are applied, then it is possible to calculate the transfer quotient (TQ) [22] and the respiratory quotient (RQ) shown in Eqs. 16 and 17 [2, 8, 12, 13, 19]

$$\text{TQ} = \frac{\text{CTR}}{\text{OTR}} \quad (16)$$

$$\text{RQ} = \frac{\text{CER}}{\text{OUR}} \quad (17)$$

The off-gas analyzer features an additional drying system within the analyzer to remove residual water from the exhaust gas stream beyond the gas cooling system.

Therefore, water is not considered in the equations presented above. The raw data were averaged over 30 values to avoid the dispersion of values and to reduce the noise.

Verification of the exhaust gas analyzer and determination of the volume-specific mass transfer coefficient for  $\text{CO}_2$

Verification was carried out using a cell-free bioreactor containing standard DMEM/Ham's F12 medium and 0.125 M citric acid, which does not damage steel and has a 97 % degree of dissociation [7]. The citric acid solution was pumped into the bioreactor at  $0.96 \text{ ml h}^{-1}$  for nearly 11 h. The anticipated CTR was  $2 \times 10^{-4} \text{ mol l}^{-1} \text{ h}^{-1}$ , and the OTR and CER were expected to be zero.

The volume-specific mass transfer coefficient for  $\text{CO}_2$  was also estimated in this experiment. The bioreactor contained two different aeration systems corresponding to gassing through the membrane into the bioreactor. The first was surface aeration, which takes place between the gas phase (headspace) and the liquid phase (medium or cell suspension) whereas the second was characterized through the transfer of gas across the membrane system [15]. Therefore, two different volume-specific transfer coefficients exist, one for surface aeration which can be estimated by using the well-known gassing out/gassing in method and one for the membrane system, which so far is only measurable using simulations [15]. For this reason, we established a new and very useful experimental procedure using our novel exhaust gas analyzing system with associated mathematical algorithm to balance the global mass transfer, introducing an all over mass transfer coefficient.

For this purpose, the liquid phase was aerated with a defined gas mixture until steady-state conditions were abandoned. Afterwards the  $\text{CO}_2$  transfer was stopped. The decreasing  $\text{CO}_2$  concentrations were monitored and used for balancing

$$\text{CT} = \text{CTR} \times t_p \quad (18)$$

The CTR values were included to determine the overall transferred  $\text{CO}_2$  (CT) at each process time interval. Then, the CTR values were averaged to avoid fluctuations.

$$\text{CT}_{n+1} = \text{CT}_n + \left( \frac{\text{CTR}_1 + \text{CTR}_2}{2} \right) \times (t_2 - t_1) \quad (19)$$

The overall transferred  $\text{CO}_2$  concentration  $\text{CT}_{n+1}$  was subtracted from the inorganic carbon concentration at the beginning of the cultivation  $c_{\text{IC},0}$ , because this  $\text{CO}_2$  had left the liquid phase

$$c_{\text{IC}} = c_{\text{IC},0} - \text{CT}_{n+1} \quad (20)$$

The current inorganic carbon concentration in the liquid phase  $c_{AC,l}$  was calculated by subtracting the  $\text{CO}_2$  concentration in the bioreactor gas phase  $c_{\text{CO}_2,g}$ .

$$c_{AC,l} = c_{AC} - c_{\text{CO}_2,g} \quad (21)$$

In the next step, the law of mass action was used to determine the ratio of  $\text{CO}_2$  to bicarbonate.

$$\frac{[\text{H}^+]}{K_S} = \frac{[\text{CO}_2]}{[\text{HCO}_3^-]} \quad (22)$$

This proportion was subsequently normalized and multiplied by the amount of inorganic carbon in the liquid phase.

$$\frac{c_{\text{CO}_2,l}}{c_{IC,l}} = \frac{\frac{[\text{CO}_2]}{[\text{HCO}_3^-]}}{1 + \frac{[\text{CO}_2]}{[\text{HCO}_3^-]}} \quad (23)$$

$$c_{\text{CO}_2,l} = \frac{c_{\text{CO}_2,l}}{c_{IC,l}} \times c_{IC,l} \quad (24)$$

Then, the temperature-corrected and substance-corrected Henry constant ( $H_S$ ) and the ambient pressure ( $p_{\text{ambient}}$ ) were used to calculate the saturation concentration of  $\text{CO}_2$  ( $c^*$ ). The saturation concentration of the gas phase depended on the bioreactor off-gas concentration  $x_{\text{CO}_2,\text{out}}$ :

$$c^* = \frac{x_{\text{CO}_2,\text{out}}}{100} \times \frac{p_{\text{ambient}}}{100} \times H_S \quad (25)$$

In the last step, the overall mass transfer coefficient  $k_{L,a}$  for  $\text{CO}_2$  was estimated using the following equation:

$$\frac{dc_L}{dt} = k_{L,a} c_{\text{CO}_2} \times (c_{\text{CO}_2,l} - c^*) \quad (26)$$

This allowed the overall mass transfer coefficient for  $\text{CO}_2$  to approximately be determined.

The global mass transfer balancing offered a  $k_{L,a}$  of oxygen of  $\sim 4.9 \text{ h}^{-1}$  in DMEM/Ham's F-12 medium and of  $\sim 4.3 \text{ h}^{-1}$  in ProCHO4 medium. The  $k_{L,a}$  of  $\text{CO}_2$  was  $\sim 2.0 \text{ h}^{-1}$  in DMEM/Ham's F-12 medium and  $\sim 2.1 \text{ h}^{-1}$  in ProCHO4 medium.

## Results and discussion

### Verification

A series of chemical verification experiments was carried out to check the system and the corresponding algorithm. A representative example is shown in Fig. 2.

Prior to the addition of citric acid, steady-state conditions were achieved as usual for mammalian cell cultivations. The added citric acid caused the pH to fall, increasing the CTR to a maximum of  $2 \times 10^{-4} \text{ mol l}^{-1} \text{ h}^{-1}$ , thus the anticipated value was achieved

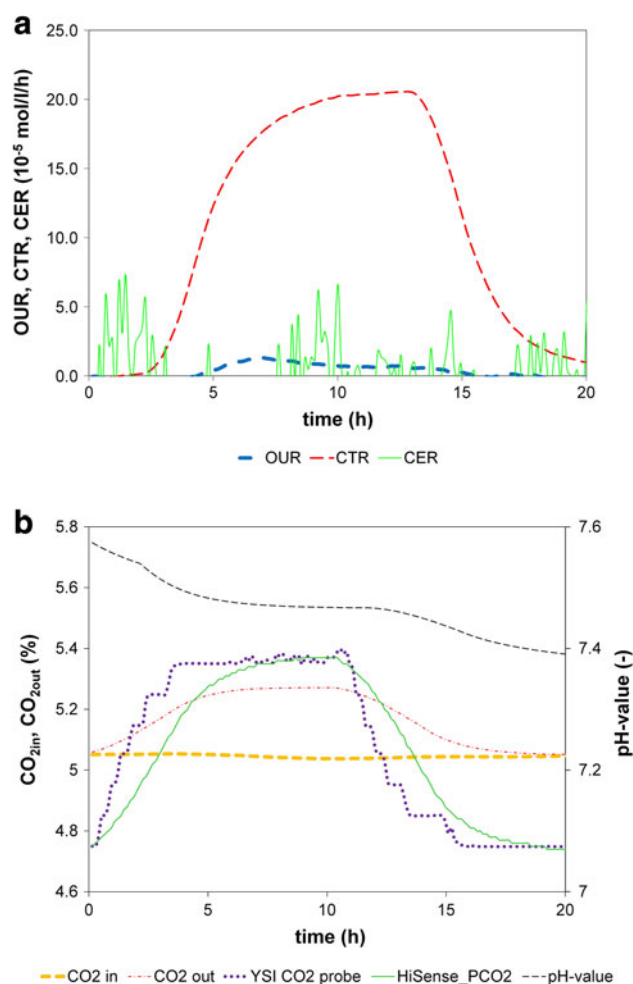


**Fig. 2** Verification experiments. Data were obtained by adding citric acid to a cell-free bioreactor containing DMEM/Ham's F12 medium under cultivation conditions. **a** During the addition of citric acid, the CTR value increased as expected. OUR and CER curves remained near zero as expected. **b** For validation, a YSI 8500 electrode in the bioreactor recorded similar values to our new analyzer and its associated algorithm

reproducibly. All the time, no dispersion in the averaged CTR signal was observed although the  $\text{CO}_2$  sensor worked at its minimum resolution. In contrast to the CTR, the OUR (identical to the OTR) and CER remained at approximately zero throughout the experiment, as expected based on a similar experiment carried out by Sperandio [26]. The algorithm correctly attributed the  $\text{CO}_2$  to the buffer, but the experiment also showed that the amplitude of noise in the CER signal was  $\sim 0.8 \times 10^4 \text{ mol l}^{-1} \text{ h}^{-1}$  in chemical simulation experiments. The CER values, therefore, had to be larger than this amplitude to distinguish between noise and a real CER signal caused by respiration of the cells. Accordingly, the quality of the CER value depended on the quality of the pH electrode, because pH was one of the main parameters characterizing the CER.

For comparison, a DCO<sub>2</sub> electrode (YSI 8500, Yellow Springs Instruments) was embedded in the bioreactor during these experiments, providing comparable values to our measuring system. The delay in acquiring the values was caused by averaging. In contrast, the probes on our analyzer were more sensitive than the YSI 8500 electrode, which offered a resolution of 0.5 % [21]. For this reason, an additional DCO<sub>2</sub> electrode for inline estimation of the CO<sub>2</sub> concentration in the liquid phase was unnecessary.

This experiment also verified the presented method used to calculate the overall mass transfer coefficient of CO<sub>2</sub>. Therefore, the equilibrium CTR, the Henry constant, the ambient pressure, the CO<sub>2</sub> concentration in the gas phase (measured and calculated with our analytical system) and the CO<sub>2</sub> concentration in the liquid phase (measured with YSI 8500) were used to calculate  $k_L a_{CO_2}$ . The result of this evaluation ( $k_L a_{CO_2} \sim 2.0 \text{ h}^{-1}$ , Fig. 3) agreed with the value determined by global mass balancing indicating that our established calculation method is suitable and accurate.

### Hybridoma cultivations

First of all, a hybridoma cell cultivation without pH and DO control is presented (Fig. 4). The CER and OUR values differed significantly in the first half of the process because of CO<sub>2</sub> release from the bicarbonate [12]. The CER, OUR and CTR increased until the culture reached its minimum pH (6.9), which indeed did not correlate with a glutamine or a glucose limitation. Both substrates were still available. Then the CER, OUR and CTR values decreased as the pH in the medium increased. Also the lactate concentration/

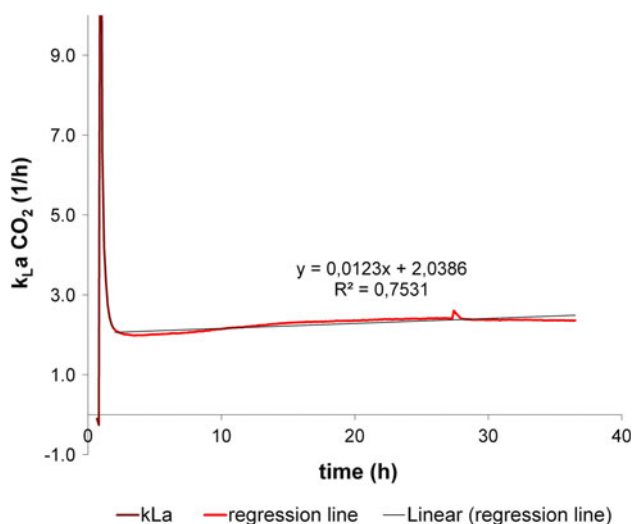


**Fig. 3** Estimation of the overall transfer coefficient in DMEM medium. The overall transfer coefficient of carbon dioxide was estimated using the graph and equations as shown

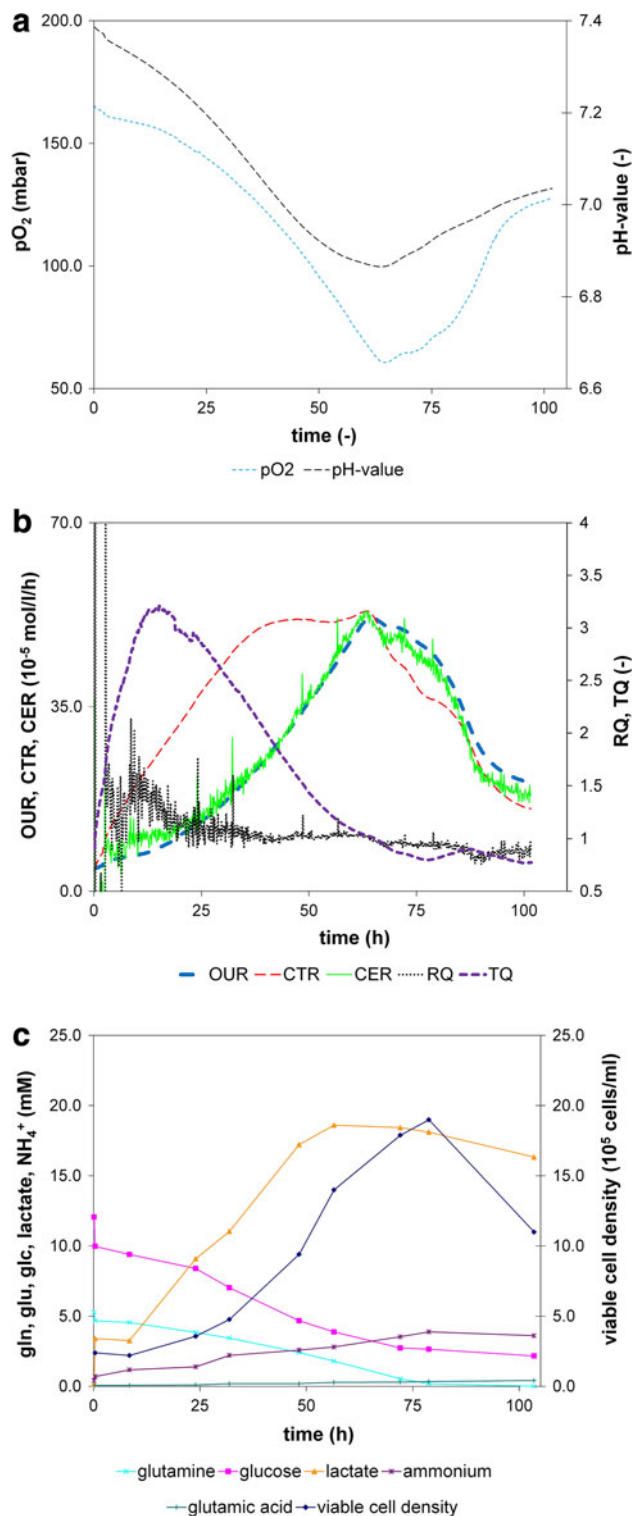


**Fig. 4** Hybridoma batch cultivation without pH and DO control. The hybridoma cells were cultivated in DMEM/Ham’s F12 medium containing 1 % FCS. The pH and DO were not controlled during this experiment because the data were used to characterize the cell line. **a** Curve progression for pH and DO. **b** Curve progression for OUR, CER, CTR, TQ and RQ. **c** Curve progression for metabolites

formation seems not to be responsible for this phenomenon because a constant lactate concentration was determined at this time point. Although the viable cell density was still increasing the values of the OUR were already decreasing, which probably means a change in metabolism should have taken place. Thereby the curve progression of the OUR agreed with mass spectrometry data reported by Behrendt [4]. A relation between the OUR profile and the viable cell density was not observed.

The RQ hovered between 1.0 and 2.0 for the first 20 h then stabilized at approximately 1.0 until the pH began to increase, whereupon it decreased to  $\sim 0.93$  and later on to  $\sim 0.88$ . No correlation between substrate consumption/product formation and the RQ value could be seen. Therefore, changes in the RQ values seem to correlate rather with the changes in the gradient of the courses (mathematical phenomenon) than with changes in metabolism.

During the hybridoma cultivation with controlled pH and DO (Fig. 5), pH control was achieved by minimizing the  $\text{CO}_2$  concentration in the feed gas stream for the first 52 h. Thereafter pH control was realized by adding NaOH. With the beginning of base addition, the CTR decreased until it equalled the CER (TQ = RQ) because no more protons reached the  $\text{NaHCO}_3$  buffer to promote the release of  $\text{CO}_2$  [2]. By 65 h, pH control was again exercised by regulating the  $\text{CO}_2$  concentration in the feed gas stream. Although glutamine was available in excess (in comparison to glucose concentration) the curve progressions of OUR, CER and accordingly the RQ were comparable to the values of the previous cultivation (without pH and DO control). In general, the signal-to-noise ratio of the CER was quite satisfactory with regard to the technical complexity of this cultivation. During the first few hours more scattered measuring values occurred reflecting low respiratory activity of the cells and  $\text{CO}_2$  addition/minimization in

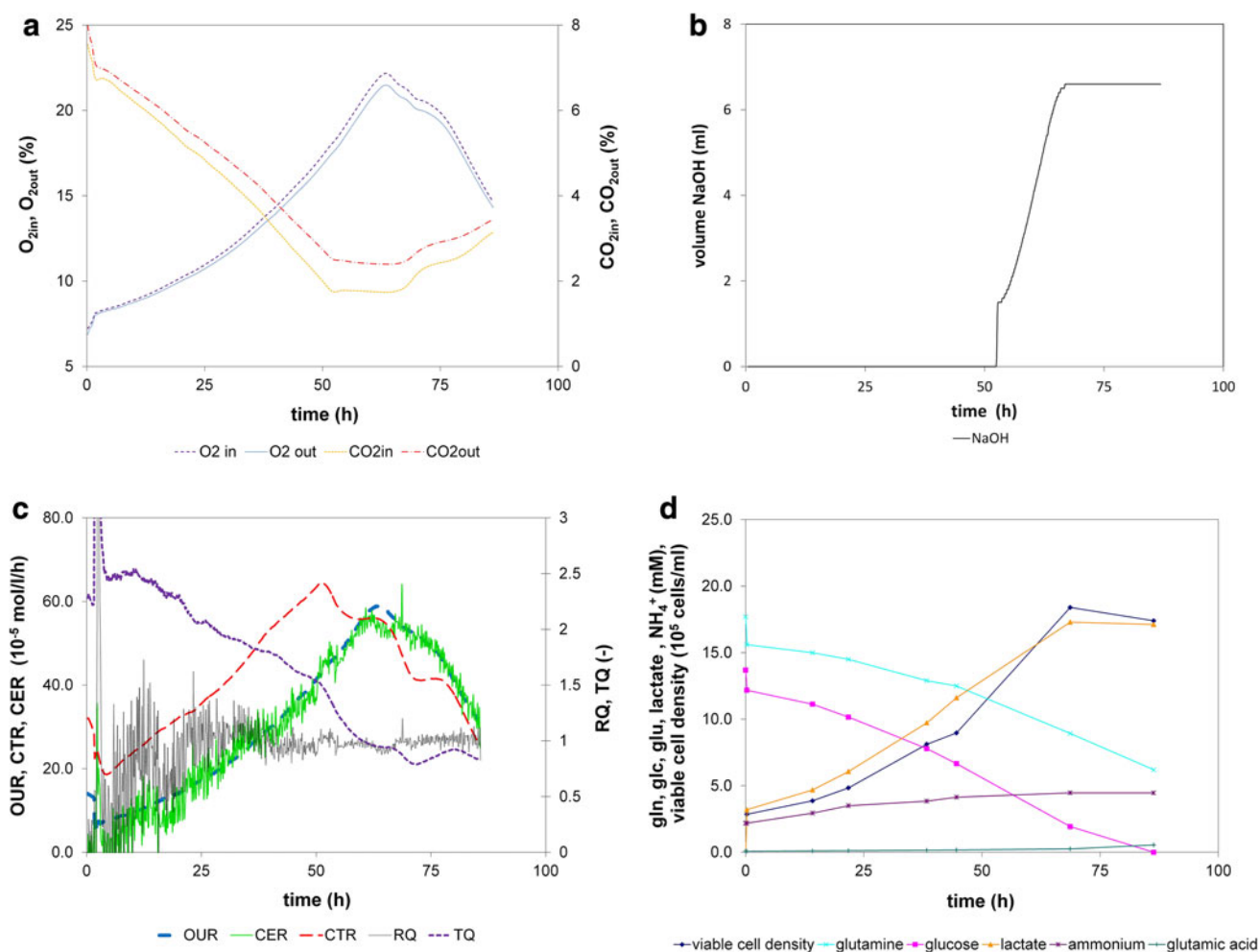


**Fig. 5** Hybridoma batch cultivation with constant pH and DO. Hybridoma cells were cultivated in DMEM/Ham's F12 medium containing 1 % FCS. The pH and DO were controlled during this experiment.  $\text{CO}_2$  and NaOH were used do keep the pH at a preset

value. **a** Course of the  $\text{CO}_2$  concentration in the inlet and off-gas streams. **b** Addition of NaOH during the fermentation. **c** Curve progression for OUR, CER, CTR, TQ and RQ. **d** Curve progression for metabolites



the feed gas stream to maintain the pH at its set point. Furthermore, a high CO<sub>2</sub> level was needed for pH control resulting in more scattered data. This was caused by the photometric working NDIR sensor which is more sensitive in the lower part (low CO<sub>2</sub> concentrations) of the measuring range than in the upper part (high CO<sub>2</sub> concentrations). In contrast to previous reports [2], the use of a mathematical algorithm allowed in-process monitoring not only when the pH was controlled by adding NaOH but also when it was controlled by CO<sub>2</sub> in the inlet gas, which is more suitable for applications in industrial processes.

DG44 cultivations

Two types of DG44 cell cultivations (without pH and DO control in PowerCHO2 medium without glutamine

supplementation) were established, which were identical apart from the aeration system (Fig. 6). Membrane aeration was used in the first process, whereas a ring sparger was embedded in the bioreactor during the second process (bubble aeration) to represent industrial applications.

The curve progressions of OUR, CER and RQ were very similar with the exception of slightly different RQ values at the beginning and more scattered measuring values in the CER signal of the membrane-aerated cultivation. The slightly different RQ values during process hour 1–20 are caused by the differences in the aeration system (membrane aeration and ring sparger). The more scattered measuring values of the membrane-aerated cultivation, however, are the consequences of suboptimal working pH electrode in evidence causing the dispersion of the CER signal.

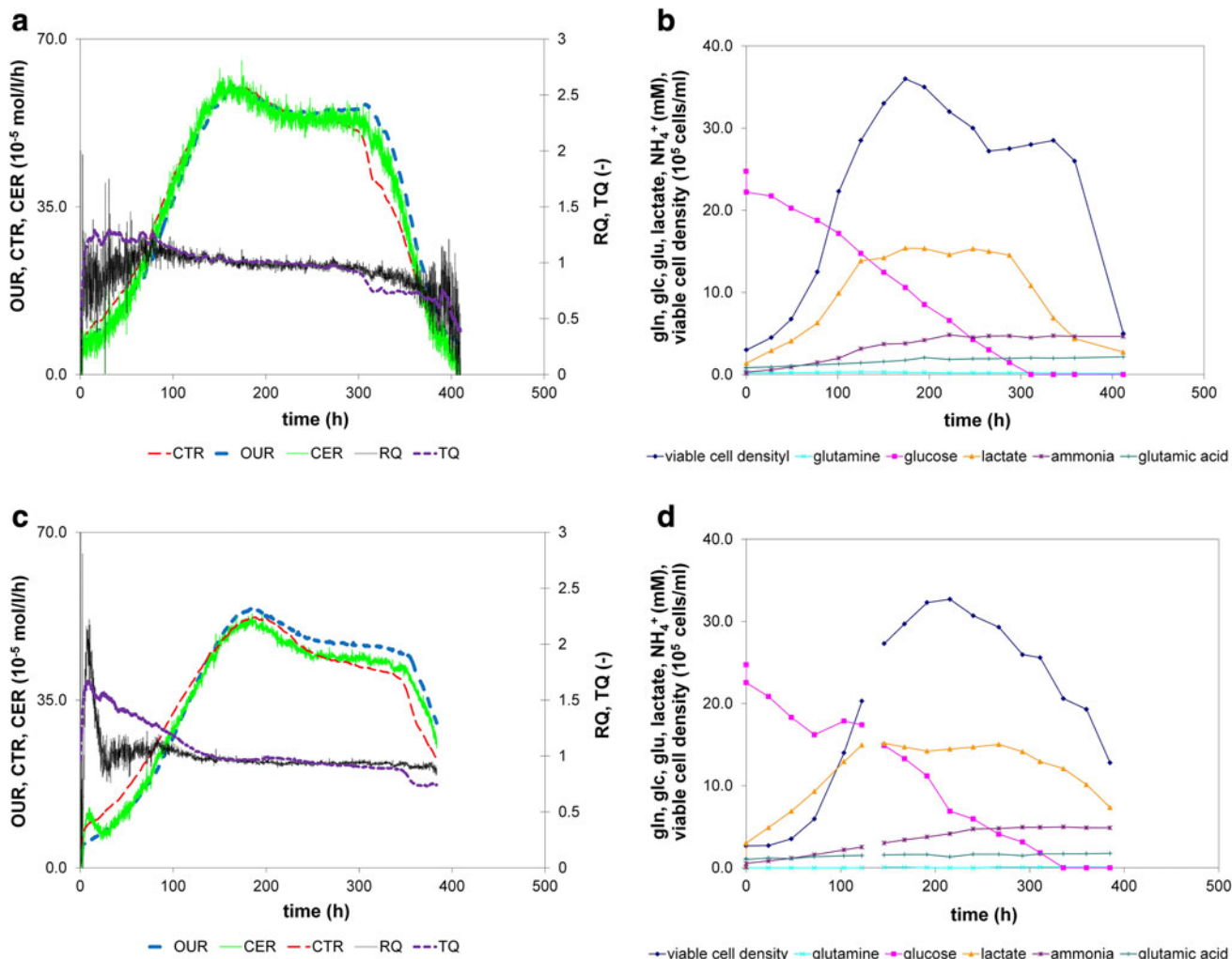


**Fig. 6** Comparison of aeration by membrane and ring sparger in batch cultivations of DG44 cells. The cells were cultivated in PowerCHO2 medium. The pH and DO were not controlled. **a** Curve progression for OUR, CER, CTR, TQ and RQ during the membrane-aerated cultivation. **b** Course of metabolites during the membrane-

aerated cultivation. **c** Curve progression for OUR, CER, CTR, TQ and RQ during the ring sparger-aerated cultivation. **d** Curve progression for metabolites during the ring sparger-aerated cultivation (one measurement value missing)

With regard to the off-line data both processes were quite comparable. The slightly lower viable cell concentration could thereby probably be caused by the bubble aeration during this cultivation. Nevertheless, the results obtained in both batch processes were very satisfying.

Another DG44 batch cultivation was performed in ProCHO4 medium (with glutamine supplementation) without pH and DO as well (Fig. 7). There the courses of OUR, CTR, CER differ remarkably in comparison to the other cultivations in PowerCHO2 medium, whereby the OUR profile was similar to the profile determined by mass spectrometry in experiments described by Haas [16].

Furthermore, also the curve progressions of the off-line measurements differ related to substrate consumption and by-product/biomass formation. In contrast to that, the RQ and TQ profiles of this batch culture were very comparable to those of the above shown cultivations. This leads to the assumption that the RQ is unsuitable for the detection of differences in the culture conditions or the cells

performances as previously suggested by Goudar [13] and Sieblist [25]. Nevertheless, an assessment of the cultures behavior is possible in comparing the respiratory activity data (OUR and CER). Changes in the culture conditions (for example the medium composition) could be detected immediately based on the OUR, CER courses. If the curve progressions offer a disagreement within different cultivations resulting in disparate OUR and CER profiles process modifications cannot only be assumed but are also most likely.

In addition, the sudden decrease behind a plateau phase of the OUR values during the DG44 cultivations indicated the limitation of glucose but did not reflect an exact relationship between the OUR profile and the viable cell density.

Last but not least a membrane-aerated fed-batch process with pH and DO control was established.

There the addition of feed solution was based on the consumption of glucose and the formation of lactate which means feeding was only valid when an oxidative glucose metabolism was observed and, therefore, NaOH supply was not required [14]. As depicted in Fig. 8, the addition of feed was not necessary during the first phase (till process hour 140) of the cultivation. Subsequently the feeding was started. Glucose was no longer traceable in the supernatant of the cell expansion, so glucose was directly metabolized. Thus, lactate formation was reduced but could not be prevented. Simultaneously the viable cell density remained constant. For this reason more feeding was allowed resulting in an increasing glucose value and an increasing cell density. Lactate formation was nearly stopped.

Up to process hour 140, the curve progressions (OUR, CER and RQ) were comparable to the previous cultivation in ProCHO4 medium due to similar cultivation conditions. With addition of feed solution changes in substrate consumption and by-product/biomass formation occurred but were not reflected in the RQ signal. On account of this, the RQ is not an appropriate parameter for the automated feedback control of a fed-batch process.

Based on the more complex cultivation conditions the dispersion of the CER values was, however, higher than in the other cultivations.

- High CO<sub>2</sub> level for pH maintenance at the beginning
- Altering culture volume
- Altering chemical conditions through feed addition
- Low viable cell density at the beginning and at the end of the cultivation

However, the obtained OUR, CER and CTR signals were very satisfying. The cultivation processes displayed measurable CER signals from a viable cell concentration of  $\sim 2 \times 10^5$  cells ml<sup>-1</sup>. Therefore our system challenged low densities well, which was important at the beginning of

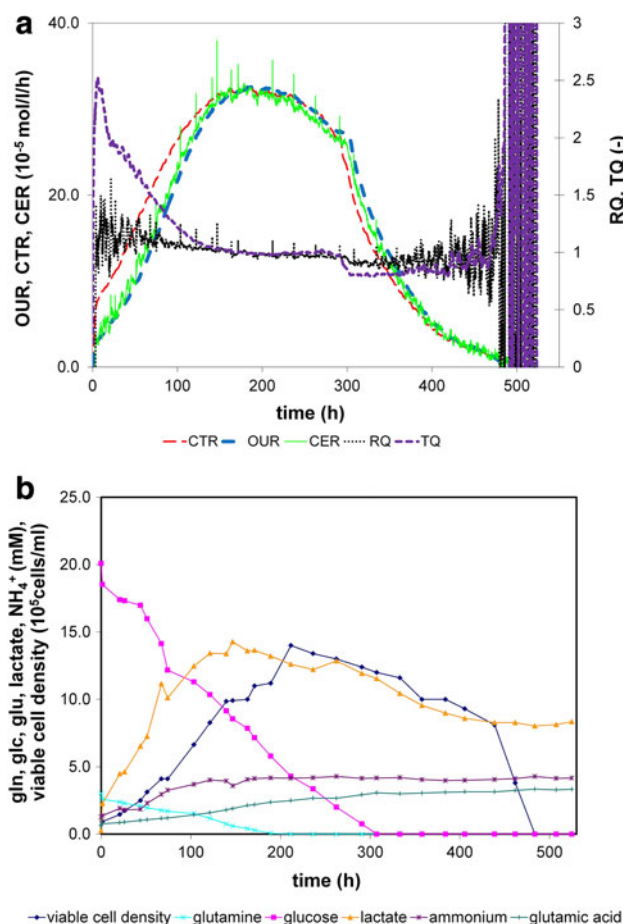


**Fig. 7** DG44 batch cultivation in ProCHO4 without constant pH and DO. The cells were cultivated in ProCHO4 medium and the pH and DO were not controlled. **a** Curve progression for OUR, CER, CTR, TQ and RQ during the membrane-aerated process. **b** Curve progression for metabolites during the membrane-aerated process

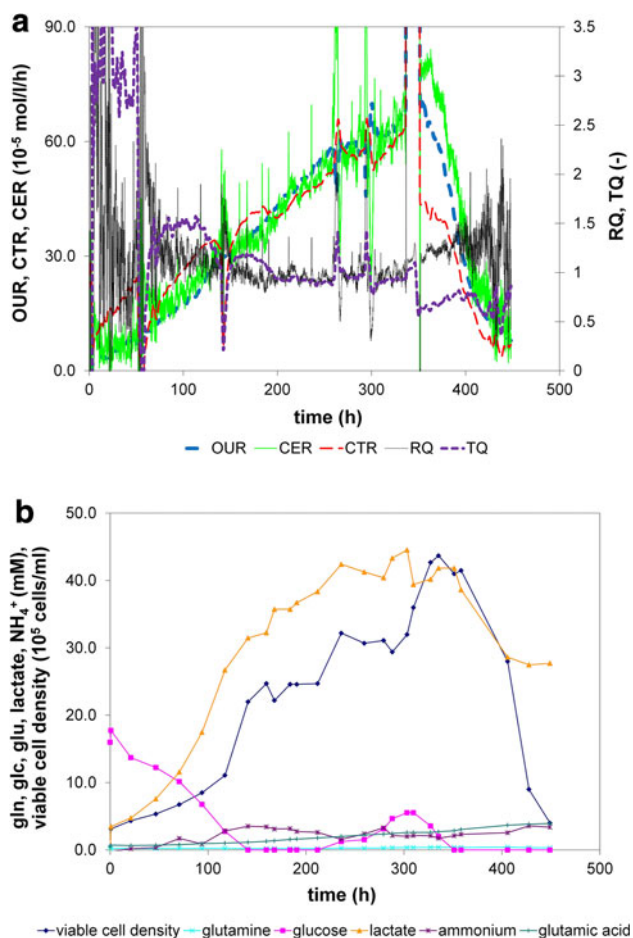


**Fig. 8** DG44 cultivation in modified ProCHO4 medium with pH and DO control. The cells were cultivated in modified ProCHO4 medium and fed with PowerFeed A solution. The pH was maintained at 7.2 and the DO at 35 % air saturation. **a** Curve progression for OUR, CER, CTR, TQ and RQ during the membrane-aerated process. **b** Curve progression for viable cell density during the membrane-aerated process

a cultivation process. The higher the cell density (greater differences in the  $O_2$  and  $CO_2$  concentrations), the better was the measured signal (OUR, CER, CTR, TQ and RQ) which means high cell densities do not pose problems. The CER peaks observed in most of the experiments were sampling artifacts for off-line analysis because the measuring system was sensitive enough to detect even minor changes in the cell culture volume.

## Conclusions

Representative experiments with two different cell lines confirmed that our developed analytical system, which combines exhaust gas analysis, inline analysis and a

corresponding algorithm, was able to determine OUR, CER, CTR, TQ and RQ values automatically and in real time, even in the presence of bicarbonate. The different cultivation set-ups yielded different CER, OUR and CTR curves but the RQ profiles were remarkably similar with shifts away from unity caused by changes to steady-state conditions as suggested by Goudar [13] and Sieblist [25]. Accordingly, the RQ signal is unsuitable for feedback control of a fed-batch process.

Unlike gas chromatography, mass spectrometry and typical off-gas analyzers, our system can estimate the CER without necessarily a transfer of an external pH signal (internal pH measurement enclosed) because it directly measures all necessary parameters. The operating costs of the novel system are lower than those of a gas chromatograph or mass spectrometer, with comparable accuracy, whereby the lower limit of the CER signal is defined through the minimum cell density if the CER signal is greater than the amplitude of noise ( $8 \times 10^{-5} \text{ mol l}^{-1} \text{ h}^{-1}$ ) at a viable cell density of  $\sim 2.0 \times 10^5 \text{ cells ml}^{-1}$ . The lower limits of the OUR and CTR are defined by the lower ranges and detection thresholds of the sensors, i.e., the more cells accumulate in the bioreactor to increase the differences between measuring points, the more accurate are the estimated OUR, CER, CTR, TQ and RQ signals. The upper limit of the system is, therefore, only defined through the upper ranges of the  $O_2$  and  $CO_2$  sensors. In addition, a high-quality and accurately calibrated pH electrode is essential because inaccurate pH values have a significant impact on the estimation of the CER (increasing noise).

The recorded data are useful to draw conclusions with respect to the batch-to-batch reproducibility of mammalian cell cultivation processes in real time, which is a key requirement under the PAT initiative. Equal curve progressions mean comparable cultivation conditions resulted in comparable outcomes. In contrast deviating charts indicate differences in the cultivation process, whereupon a root cause analysis is necessary. Because the culture conditions are monitored constantly, all process modes can be used (manuscript including perfusion is in preparation) whether or not the pH and DO are controlled. The new system was shown to be precise, reliable (low maintenance) and low-wear (only one broken magnetic valve during the development and experimental period) even in the challenging environment of a membrane-aerated cultivation process. Therefore, the system could become an important component to investigate the reproducibility of biopharmaceutical manufacturing processes to ensure that the process meets GMP guidelines.

**Acknowledgments** This project was funded by MWEIMH of Germany with encouragement of the European Union.

## References

- Aehle M, Kuprijanov A, Schaepe S, Simutis R, Lübbert A (2011) Increasing batch-to batch reproducibility of CHO cultures by robust open-loop control. *Cytotechnology* 63(1):41–47
- Aehle M, Kuprijanov A, Schaepe S, Simutis R, Lübbert A (2011) Simplified off-gas analyses in animal cell cultures for process monitoring and control purposes. *Biotechnol Lett* 33(11):2103–2110
- Aiba S, Furuse H (1990) Some comments on respiratory quotient (RQ) determination from the analysis of exit gas from a fermentor. *Biotechnol Bioeng* 36(5):534–538
- Behrendt U, Koch S, Gooch DD, Steegmans U, Comer MJ (1994) Mass spectrometry: a tool for on-line monitoring of animal cell culture. *Cytotechnology* 14:157–165
- Binder H, Buchholz K, Deckwer WD, Hustedt H, Kroner KH, Kula MR, Quicker G, Schumpe A, Wiesmann U (1982) *Reaction-Engineering*. Springer, Heidelberg
- Bliefert C (1978) pH measurements. Publishing company chemistry, UK
- Bloemen HHJ, Wu L, van Gulik WM, Heijnen JJ, Verhaegen MHG (2003) Reconstruction of the O<sub>2</sub> uptake rate and CO<sub>2</sub> evolution rate on a time scale of seconds. *AIChE J* 49(7):1895–1908
- Bonarius HP, de Gooijer CD, Tramper J, Schmid G (1995) Determination of the respiration quotient in mammalian cell culture in bicarbonate buffered media. *Biotechnol Bioeng* 45(6):524–535
- Deckwer W, Schumpe A (1978) Estimation of O<sub>2</sub> and CO<sub>2</sub> solubilities in fermentation media. *Biotechnol Bioeng* 21:1075–1078
- Ducommun P, Ruffieux P, Furter M, Marison I, von Stockar U (2000) A new method for on-line measurement of the volumetric oxygen uptake rate in membrane aerated animal cell cultures. *J Biotechnol* 78(2):139–147
- FDA (2004) Guidance for Industry. PAT- A Framework for Innovative Pharmaceutical Development, Manufacturing, and Quality Assurance
- Frahm B, Blank HC, Cornand P, Oelssner W, Guth U, Lane P, Munack A, Johannsen K, Portner R (2002) Determination of dissolved CO<sub>2</sub> concentration and CO<sub>2</sub> production rate of mammalian cell suspension culture based on off-gas measurement. *J Biotechnol* 99(2):133–148
- Goudar CT, Piret JM, Konstantinov KB (2011) Estimating cell specific oxygen uptake and carbon dioxide production rates for mammalian cells in perfusion culture. *Biotechnol Prog* 27(5):1347–1357
- Hass VC, Pörtner R (2009) *Practice of bioprocess engineering. With virtually practical training*. Spektrum Akad. Verl, Heidelberg
- Henzler H, Kauling DJ (1993) Oxygenation of cell culture. *Bioproc Eng* 9:61–75
- Haas J (2010) Online determination of oxygen uptake and carbon dioxide production rates in mammalian cell culture using mass spectrometry. *Cells and culture/proceedings of the 20th ESACT meeting, Dresden, Thomas Noll ed. Cells and culture, Esact Proceedings*, 4: 683–687
- Junker B, Wang H (2006) Bioprocess monitoring and computer control: key roots of the current PAT initiative. *Biotechnol Bioeng* 95(2):226–261
- Lovrecz G, Gray P (1994) Use of on-line gas analysis to monitor recombinant mammalian cell cultures. *Cytotechnology* 14(3):167–176
- Neeleman R, van den End EJ, van Boxtel AJ (2000) Estimation of the respiration quotient in a bicarbonate buffered batch cell cultivation. *J Biotechnol* 80(1):85–94
- Oezemre A, Heinzle E (2001) Measurement of oxygen uptake and carbon dioxide production rates of mammalian cells using membrane mass spectrometry. *Cytotechnology* 37(3):153–162
- Pattison RN, Swamy J, Mendenhall B, Hwang C, Frohlich BT (2000) Measurement and control of dissolved carbon dioxide in mammalian cell culture processes using an in situ fiber optic chemical sensor. *Biotechnol Prog* 16(5):769–774
- Royce PN (1992) Effect of changes in the pH and carbon dioxide evolution rate on the measured respiratory quotient of fermentations. *Biotechnol Bioeng* 40(10):1129–1138
- Royce PN, Thornhill NF (1991) Estimation of dissolved carbon dioxide concentrations in aerobic fermentations. *AIChE J* 37(11):1680–1686
- Schumacher W, Leonhard W (2001) Basic information of automatic control engineering
- Sieblist C, Jenzsch M, Pohlscheidt M, Lübbert A (2011) Insights into large-scale cell-culture reactors: i. Liquid mixing and oxygen supply. *Biotechnol J* 6(12):1532–1546
- Sperandio M (1997) Determination of carbon dioxide evolution rate using on-line gas analysis during dynamic biodegradation experiments. *Biotechnol Bioeng* 53(3):243–252
- Stumm W, Morgan JJ (1996) *Aquatic chemistry*. Wiley and sons, New York
- Whitford W, Julien C (2007) Analytical technology and PAT. *Bio Process Intern (Supplement)*:32–41
- Wu L, Lange HC, van Gulik WM, Heijnen JJ (2003) Determination of in vivo oxygen uptake and carbon dioxide evolution rate from off-gas measurements under highly dynamic conditions. *Biotechnol Bioeng* 81(4):448–458